Steady-State Antigen Scavenging, Cross-Presentation, and CD8$^+$ T Cell Priming: A New Role for Lymphatic Endothelial Cells

Sachiko Hirosue,*[,1] Efthymia Vokali,*[,1] Vidya R. Raghavan,* Marcela Rincon-Restrepo,* Amanda W. Lund,* Patricia Corthésy-Henrioud,* Francesca Capotosti,* Cornelia Halin Winter,[†] Stéphanie Hugues,[‡] and Melody A. Swartz*[,§]

Until recently, the known roles of lymphatic endothelial cells (LECs) in immune modulation were limited to directing immune cell trafficking and passively transporting peripheral Ags to lymph nodes. Recent studies demonstrated that LECs can directly suppress dendritic cell maturation and present peripheral tissue and tumor Ags for autoreactive T cell deletion. We asked whether LECs play a constitutive role in T cell deletion under homeostatic conditions. In this study, we demonstrate that murine LECs under noninflamed conditions actively scavenge and cross-present foreign exogenous Ags to cognate CD8$^+$ T cells. This cross-presentation was sensitive to inhibitors of lysosomal acidification and endoplasmic reticulum–golgi transport and was TAP1 dependent. Furthermore, LECs upregulated MHC class I and the PD-1 ligand PD-L1, but not the costimulatory molecules CD40, CD80, or CD86, upon Ag-specific interactions with CD8$^+$ T cells. Finally, Ag-specific CD8$^+$ T cells that were activated by LECs underwent proliferation, with early-generation apoptosis and dysfunctionally activated phenotypes that could not be reversed by exogenous IL-2. These findings help to establish LECs as APCs that are capable of scavenging and cross-presenting exogenous Ags, in turn causing dysfunctional activation of CD8$^+$ T cells under homeostatic conditions. Thus, we suggest that steady-state lymphatic drainage may contribute to peripheral tolerance by delivering self-Ags to lymph node–resident leukocytes, as well as by providing constant exposure of draining peripheral Ags to LECs, which maintain tolerogenic cross-presentation of such Ags. ***The Journal of Immunology*****, 2014, 192: 5002–5011.**

The lymphatic system transports interstitial fluid, Ags, solutes, and immune cells from the periphery and returns them to the blood circulation after surveillance through lymph nodes (LNs), thereby initiating adaptive immune responses (1–3). In addition to effector immune responses, LNs are important sites for the maintenance of peripheral tolerance. LN stromal cells, which include lymphatic endothelial cells (LECs) and blood endothelial cells (BECs), as well as fibroblastic reticular cells (FRCs) in the T cell zone, are thought to contribute to tolerance induction of autoreactive T cells that escape central memory (4), as well as regulate the contraction of inflammatory responses (5). Indeed, the lymphatic endothelium is emerging as an important player in shaping immunity and tolerance (1–3, 6–10). For example, LECs were shown to suppress maturation of dendritic cells (DCs) (1, 4, 11) and their subsequent priming of CD8$^+$ T cells in a contact-dependent manner (4, 5, 9). In addition, LECs, as well as FRCs, can directly prime CD8$^+$ T cells (5); they express components of the Ag-presentation machinery, including MHC class I and II molecules (6–9, 12), and were shown to directly contribute to peripheral tolerance by expression and presentation of endogenous peripheral tissue Ags (PTAs), leading to compromised CD8$^+$ T cell activation (6–9). They are also sensitive to pathogen-associated molecular patterns via the expression of various members of the TLR family (8, 11). Together, these studies established LECs as contributors to the maintenance of peripheral tolerance to endogenously expressed self-Ags.

However, little is known about whether LECs as APCs have the ability to capture and process exogenous Ags for CD8$^+$ T cell deletion. Although so-called "professional" APCs, such as CD8a$^+$ DCs, can process exogenous Ags for cross-presentation to CD8$^+$ T cells, some nonhematopoietic cell types also were shown to be capable of cross-presentation (13). For example, liver sinusoidal endothelial cells (LSECs) are thought to capture and cross-present circulating Ag to CD8$^+$ T cells, leading to CD8$^+$ T cell deletion and the establishment of a tolerogenic environment (14). This is especially important in the liver, where LSECs are among the first cells to encounter the large diversity of foreign Ags from food, as well as TLR agonists from commensal sources (15).

*Institute of Bioengineering, Ecole Polytechnique Fédérale de Lausanne, 1015 Lausanne, Switzerland; [†]Institute of Pharmaceutical Sciences, Swiss Federal Institute of Technology Zürich (ETHZ), Zürich, Switzerland; [‡]Department of Pathology and Immunology, Faculty of Medicine, Centre Médical Universitaire, Université de Genève, Geneva, Switzerland; and [§]Swiss Institute for Experimental Cancer Research, Ecole Polytechnique Fédérale de Lausanne, 1015 Lausanne, Switzerland

[1]S. Hirosue and E.V. contributed equally to this work.

Received for publication September 16, 2013. Accepted for publication March 29, 2014.

This work was supported by the Swiss National Science Foundation (31-135756 to M.A.S.), the European Research Commission (323053 to M.A.S. and 281365 to S. Hugues), and the Leenaards Foundation (to M.A.S. and S. Hugues). V.R.R. was funded by a Fulbright scholarship.

Address correspondence and reprint requests to Prof. Melody A. Swartz, Institute of Bioengineering, SV-IBI-LLCB, Station 15, École Polytechnique Fédérale de Lausanne, 1015 Lausanne, Switzerland. E-mail address: melody.swartz@epfl.ch

The online version of this article contains supplemental material.

Abbreviations used in this article: BEC, blood endothelial cell; BFA, brefeldin A; BMDC, bone marrow–derived dendritic cell; COVA$_{250–264}$, Cys-OVA$_{250–264}$; DC, dendritic cell; ER, endoplasmic reticulum; FRC, fibroblastic reticular cell; i.d., intradermal(ly); iLEC, immortalized dermal lymphatic endothelial cell; LEC, lymphatic endothelial cell; LN, lymph node; LSEC, liver sinusoidal endothelial cell; NP, nanoparticle; OVA-AF647, OVA labeled with Alexa Fluor 647; PTA, peripheral tissue Ag; WT, wild-type.

Similarly, LECs are the first cells to contact extracellular Ags that arise in the periphery and drain into lymphatic vessels after, for example, tissue damage, inflammation, or infection. We recently showed that a foreign Ag (OVA) expressed by an orthotopically implanted tumor could be cross-presented by tumor-associated LECs that, when isolated, could drive dysfunctional activation of cognate $CD8^+$ T cells and promote tumor progression (16). Because tumors use physiological mechanisms to promote tolerance for their survival (17), we hypothesized that a similar mechanism of Ag cross-presentation by LECs may exist under steady-state conditions to promote tolerance against self-Ags.

In this article, we demonstrate that, under homeostatic conditions, LECs constitutively uptake and cross-present exogenous Ags to $CD8^+$ T cells. We further show that LEC-activated T cells are more rapidly apoptotic, upregulate so-called "exhaustion markers" (PD-1, CTLA-4, and CD80), secrete less IFN-γ and IL-2, and express lower levels of the activation markers CD25, CD44, and CD69 compared with T cells activated by mature DCs. Together, these data suggest that LECs help to maintain $CD8^+$ T cell tolerance to exogenous Ags that are encountered in lymph under steady-state conditions, which may be important for preventing autoimmune reactions against self-Ags after infection or injury.

Materials and Methods

Reagents

All chemicals were from Sigma-Aldrich (Buchs, Switzerland), unless otherwise noted. The mature MHC class I epitope, $OVA_{256–264}$ (SIINFEKL) peptide, was from GenScript (Piscataway, NJ). Endotoxin-free OVA was from Hyglos (Bernried am Starnberger See, Germany). Abs used in flow cytometry were from eBioscience (Vienna, Austria) or BioLegend (Lucerne, Switzerland) unless otherwise noted.

Mice

The following mice strains were used in this study at age 6–12 wk, unless noted otherwise. Female C57BL/6 wild-type mice and OT-I–transgenic mice, C57BL/6- Tg(TcraTcrb)1100Mjb/J, were purchased from Harlan Laboratories (Gannat, France). $TAP1^{-/-}$ mice (B6.129S2-*Tap1tm1Arp*/J) were purchased from The Jackson Laboratory (Farmington, CT). Animals were housed in pathogen-free facilities, and all procedures were approved by the Cantonal Veterinary Committee of Vaud, Switzerland (Protocol number 2518).

Cell lines

Conditionally immortalized dermal LECs (iLECs; Immortomice) were isolated and cultured as previously described (18). Cell culture surfaces used in all assays were coated with collagen (10 μg/ml PureCol; Advanced Biomatrix, San Diego, CA) and 10 μg/ml human fibronectin (Millipore, Billerica, MA) prior to seeding. Cells were grown in 40% DMEM low glucose, 40% F12, 20% FBS (all from Invitrogen, Zug, Switzerland), supplemented with 10 μg/ml native bovine endothelial mitogen (AbD Serotec, Düsseldorf, Germany) and 56 μg/ml heparin sodium salt from porcine intestinal mucosa (Sigma-Aldrich). To induce large T Ag expression, IFN-γ (R&D Systems, Abingdon, U.K.) was added to the media at 100 U/ml, and cells were propagated at 33°C. Prior to all experiments, cells were grown for 72 h in the absence of IFN-γ at 37°C and maintained as such.

Primary cell isolation

To obtain primary LN LECs, LNs were digested with 0.25 mg/ml Liberase DH and 100 μg/ml DNase (both from Roche, Basel, Switzerland) to obtain a single-cell suspension and cultured as described (19). Cells were cultured for 5 d until confluent; removed by Accutase (Biological Industries, Lucerna-Chem, Lucerne, Switzerland); stained with mAbs against gp38 (clone 8.1.1), CD31 (clone 390), and CD45 (clone 30-F10); and FACS sorted (FACSAria II; BD, Basel, Switzerland) into the following subpopulations, as described (20): FRCs ($gp38^+CD31^-$), LECs ($gp38^+CD31^+$), BECs ($gp38^-CD31^+$), and double-negative cells ($gp38^-CD31^-$). Bone marrow–derived DCs (BMDCs) were harvested from C57BL/6 mice, differentiated in GM-CSF as described (21), and used at day 7 of culture.

Synthesis of peptide-conjugated nanoparticles

To explore the mechanisms of cross-presentation, poly (propylene sulfide) nanoparticles (NPs) with ∼30 nm diameter were synthesized and characterized as described (22). The long peptide containing the mature MHC class I epitope SIINFEKL–Cys-$OVA_{250–264}$ ($COVA_{250–264}$) was synthesized in-house and activated with a 2-pyridylthiol, as previously described (22). Core sulfhydryls on NPs were reacted with the activated peptide to achieve conjugation of the peptide to the NPs (NP-ss-$COVA_{250–264}$) via a reducible disulfide bond (-ss-) and purified on a Sepharose CL6B column (Sigma-Aldrich). To fluorescently label the NPs, they were exposed to Dy-649 maleimide (Dyomics, Jena, Germany) after dialysis in a 1:60 molar ratio of dye/NP sulfydryl groups in PBS at room temperature for 24 h (22). Free dye was removed by gel filtration, as above, but in endotoxin-free water (B. Braun Medical, Sempach, Switzerland) as eluent. Endotoxin levels of Ags were routinely assessed by a colorimetric assay based on the HEK-Blue TLR4 cell line (InvivoGen, San Diego, CA), according to the manufacturer's protocol using a standard curve generated from the E-Toxate endotoxin standard (Sigma-Aldrich).

In vivo Ag drainage

To determine whether LN LECs can actively capture Ags in vivo, we injected fluorescently labeled OVA protein into the limbs of mice and determined its distribution within various cells in the LN after 90 min. Endotoxin-free OVA was labeled with Alexa Fluor 647 NHS (OVA-AF647; Dyomics) and purified by size-exclusion chromatography using a Sephadex G-25 column with PBS as eluent. C57BL/6 mice were injected intradermally (i.d.) with 15 μg OVA-AF647 in the limbs. After 90 min, mice were transcardially perfused with a heparinized saline solution containing 1 g/l glucose and 20 mM HEPES (pH 7.2). For immunostaining, brachial LNs were removed and fixed overnight in 2% paraformaldehyde in PBS (pH 7.4). After three washes in PBS, LNs were embedded in a block of 2% agarose and sectioned (150 μm) using a using a vibratome (Leica, Wetzlar, Germany). Sections were blocked in 0.5% of casein and further labeled using Abs against CD3ε (BD Pharmingen; clone 500A2) and LYVE-1 (Reliatech, San Pablo, CA). Images were acquired on a Leica SP5 confocal microscope using a 20× or 60× objective and processed using Imaris software (Bitplane, Zürich, Switzerland). For flow cytometric analysis, brachial LNs from individual mice were pooled and digested with 1 mg/ml Collagenase D and 200 Kunitz/ml DNase I (Sigma-Aldrich). After LNs were fully digested, as described (19), the single-cell preparations were enriched for nonhematopoietic stromal cells by CD45 cell depletion using CD45 MicroBeads (Miltenyi Biotec, Bergisch Gladbach, Germany). Enriched stroma and the $CD45^+$ fraction were counted, stained with gp38, CD31, CD45, and LYVE-1 and CD45, CD11c, CD11b, and MHC class II, respectively, and analyzed by flow cytometry (CyAn ADP Flow Cytometer; DAKO). Data analysis was performed using FlowJo software v9.2 (TreeStar, Ashland, OR).

Intracellular localization studies

To determine the intracellular pathways of Ag trafficking, we incubated iLECs with fluorescently labeled OVA and stained for different cellular components. Cells were seeded on glass coverslips (15 mm round; Karl Hecht, Sondheim, Germany), coated as above, at 2×10^5 cells/well in 12-well plates. NP-Dy649 or OVA-AF647, at a final concentration of no more than 5 mg/ml or 10 μg /ml, respectively, was added to the cells for 1 h on ice in buffered (25 mM HEPES) reduced serum (2% FBS) culture media and then transferred to 37°C for 15 or 90 min. Cells were fixed in 4% paraformaldehyde in PBS and permeabilized in permeabilization buffer (3% BSA and 0.1% saponin) in PBS overnight at 4°C. Primary Ab incubations were for 1 h, followed by species-matched secondary Abs for 30 min at room temperature. The sample was stained for clathrin at 15 min or for LAMP-1 at 90 min. All Ab dilutions were made in permeabilization buffer. Coverslips were mounted with Citifluor (Citifluor, London, U.K.) and imaged with a 63× oil-immersion lens on an LSM 700 inverted confocal microscope (Carl Zeiss, Feldbach, Switzerland). After image deconvolution (Huygens Deconvolution software; Scientific Volume Imaging, The Netherlands), Fiji software (National Institutes of Health, Bethesda, MD) with the Image 5D plugin was used to generate the figures. To quantify fluorescent NP or OVA colocalization within clathrin-positive vesicles, single z-planes from deconvolved images were analyzed using a script that determines the statistical significance of object-based colocalization by comparison of the colocalization occurrences on actual images with colocalization by chance (23). The ImarisXT MATLAB plugin "split spots onto surface objects" was used to determine whether NP^+ or OVA^+ spots were within or outside of $LAMP\text{-}1^+$ surfaces. Spots were defined as ≤0.2 μm in diameter, and $LAMP\text{-}1^+$ surfaces were drawn within a reso-

lution of 0.1 μm from the immunofluorescence signal. Intravesicular spots were defined as spots within this surface.

In vitro Ag cross-presentation

To determine whether LECs can cross-present Ag in vitro, cells were plated at 5×10^4/well in 24-well plates and stimulated with 2.5 μM $OVA_{257–264}$ (SIINFEKL), 2.5 μM NP-ss-$COVA_{250–264}$, or equivalent concentrations of unconjugated NP for 18 h in medium buffered with 25 mM HEPES (pH 7.4) at 4 or 37˚C. Cell surface H2-K^b–$OVA_{257–264}$ complexes were detected with the Ab 25d1.16 using flow cytometry. To characterize the kinetics of OVA accumulation in LECs, cells were stimulated with 1 μM OVA-AF647 for up to 90 min, washed, and analyzed for OVA uptake by flow cytometry. To demonstrate $CD8^+$ T cell priming, APCs were seeded at 10^4 cells/well in 96-well round-bottom (BMDC) or flat-bottom (LEC) plates.

In vitro T cell coculture assays

To determine the outcome of $CD8^+$ T cell interaction with cross-presenting LECs, we performed coculture assays. $CD8\alpha^+$ T cells were purified from the spleen of an OT-I mouse by negative selection (CD8α Kit II; Miltenyi Biotec). For LEC–T cell or DC–T cell coculture studies, 10^4 LECs or DCs were cocultured with naive $CD8^+$ T cells from OT-I mice (1:10 ratio) in 96-well plates for 72 h in 200 μl coculture media (IMDM with 10% FBS and 1% penicillin/streptomycin). To inhibit Ag uptake and processing, cells were treated with dynasore, LY294002, or lactacystin (inhibitors of dynamin, PI3K, and proteasome activity, respectively) 1 h prior to addition of Ag (SIINFEKL or NP-ss-$COVA_{250–264,}$ 1 nM peptide concentration) in APC-specific media. For drugs that inhibit intracellular Ag trafficking, we applied the Ag for 1 h prior to addition of brefeldin A (BFA) and chloroquine, which inhibit protein transport from the endoplasmic reticulum (ER) to the golgi apparatus and endosome acidification, respectively. After 24 h of incubation at 37˚C, cells were washed and fixed with 2% paraformaldehyde in PBS (pH 7.4) for 10 min on ice. After washing, CFSE-labeled $CD8^+$ OT-I T cells were added as above. Supernatants were harvested and frozen for cytokine analysis by ELISA (R&D Systems, Minneapolis, MN). Cells were then processed and stained for immunological markers to be analyzed by flow cytometry. Cellular proliferation was monitored by CFSE dilution, and apoptosis was determined by annexin V staining (BioVision, Milpitas, CA). OT-I T cell proliferation was determined by assessing CFSE intensity using the automated tool in FlowJo 9.4.11 and is reported as a division index (i.e., the average number of divisions that a cell has undergone). Division index = (proliferation index [average number of divisions] × percentage of dividing cells). Intracellular IFN-γ was determined after 2 h of PMA/ionomycin treatment and 2 h of BFA treatment. In some experiments, coculture media were supplemented with 50 U/ml IL-2 (Roche, Mannheim, Germany) media to determine the effect of exogenous IL-2 on LEC–T cell interactions.

Statistical analysis

Statistical analysis was performed using one-way ANOVA, followed by the Bonferroni posttest, with Prism software (GraphPad, San Diego, CA) unless otherwise stated. Results are shown as mean ± SD, with significance indicated as $*p \leq 0.05$, $**p \leq 0.01$, and $***p \leq 0.001$.

Results

LECs scavenge exogenous Ag in vivo and in vitro

Although LECs transport Ags from the periphery to the lymph, we asked whether they also could scavenge and process Ags. To this end, we injected fluorescently labeled OVA protein (OVA-AF647) i.d. in the forearm and observed its distribution in the brachial-draining LNs after 90 min. The use of a foreign protein allowed us to determine specifically the immune response against an exogenous versus self-expressed PTA. Using confocal microscopy of thick sections of the brachial LN, we observed OVA in the lymphatic-rich, LYVE-1^+ sinuses of the LN (Fig. 1A). Upon magnification of the LYVE-1^+ regions, we observed that much of the OVA was contained within LYVE-1^+ cells, suggesting intracellular accumulation in LECs (Fig. 1B, 1C). Flow cytometric analysis validated the observed scavenger activity and demonstrated that LN LECs ($CD45^-gp38^+CD31^+$LYVE-1^+ cells), as well as professional APCs, contained soluble OVA (Fig. 1D, 1E, Supplemental Fig. 1). Among the $CD45^-$ stromal cells, LECs took up the most OVA (50 ± 8%). When considered as a percentage of each cell population that took up OVA, LECs were on par with DCs for their scavenging ability (30 ± 20% versus 30 ± 5%, respectively).

In vitro, we could follow the accumulation of fluorescent OVA by iLECs (18). The degree of OVA-AF647 accumulation by iLECs was similar to that of BMDCs over 90 min at 37˚C, reaching a plateau within 40 min, as observed by flow cytometry (Fig. 1F, 1G, Supplemental Fig. 1C). This exogenous Ag uptake was an active or energy-dependent process, because OVA uptake at 4˚C by iLECs was minimal compared with that at 37˚C (Fig. 1G, Supplemental Fig. 1D). These results confirm that exogenous proteins are actively scavenged by LECs, both in vivo and in vitro.

LECs process and route Ag for cross-presentation on MHC class I in a TAP1-dependent manner

Accumulation of exogenous proteins inside LECs allows for the possibility of Ag processing and cross-presentation on MHC class I by these cells. We asked whether hallmarks of cross-presentation could be observed in LECs under controlled in vitro conditions.

First, we determined whether uptake of exogenous Ags could lead to peptide loading onto MHC class I molecules and presentation on the cell surface by immunostaining cells with the mAb 25d1.16, which specifically binds the MHC class I–bound $CD8^+$ dominant epitope of OVA, SIINFEKL ($OVA_{257–264}$). To avoid SIINFEKL peptide binding directly to surface MHC class I, and thus bypass the need for intracellular processing and cross-presentation, we used a N-terminally elongated SIINFEKL peptide conjugated onto synthetic poly(propylene sulfide) 30-nm NPs, a tool that we recently developed in our laboratory for more efficient SIINFEKL/MHC class I cross-presentation by 25d1.16 compared with OVA (22). Although SIINFEKL peptide can bind to MHC class I without cell internalization and processing, this 16-aa peptide on the NPs (NP-ss-$COVA_{250–264}$) minimally binds to surface MHC class I; instead, it requires uptake and intracellular processing for MHC class I loading in BMDCs (22). Exogenously applied NP-ss-$COVA_{250–264}$ resulted in the detection of MHC class I peptide complexes in an energy-dependent manner in both iLECs and ex vivo–cultured primary LN LECs (Fig. 2A, 2B). By conducting this study at both 4 and 37˚C, we confirmed that the cross-presentation of NP-ss-$COVA_{250–264}$ by LECs requires active processing, because cells that received SIINFEKL, but not NP-bound peptide Ag, showed elevated 25d1.16 staining at 4˚C (Fig. 2A, 2B).

We then applied inhibitors of Ag uptake and intracellular trafficking to elucidate the relevant steps in LEC cross-presentation. We cocultured inhibitor-treated, Ag-loaded LECs with OT-I $CD8^+$ T cells and assessed T cell proliferation by CFSE dilution as a measure of MHC class I/SIINFEKL presentation on the LEC surface. To confirm that LEC-induced T cell stimulation was dependent on intracellular uptake of NP-ss-$COVA_{250–264}$, we pretreated iLECs with dynasore, an inhibitor of dynamin that affects both clathrin- and caveolin-mediated uptake (24), or LY294002, a PI3K inhibitor that affects macropinocytosis (25). Both inhibitors led to reduced OT-I T cell proliferation in a concentration-dependent manner when LECs were treated with NP-conjugated Ag, but not free SIINFEKL peptide (Fig. 2C), confirming active uptake mechanisms contributing to MHC class I presentation.

We next asked whether intracellular transport processes were important in LEC cross-presentation. To this end, we treated iLECs with BFA, which inhibits Ag transport from the ER to golgi (26), or chloroquine, which inhibits acidification and vesicle fusion to late endosomes/lysosomes (27). When LECs were pretreated with either of these agents, it also resulted in concentration-dependent inhibition of T cell proliferation (Fig. 2C).

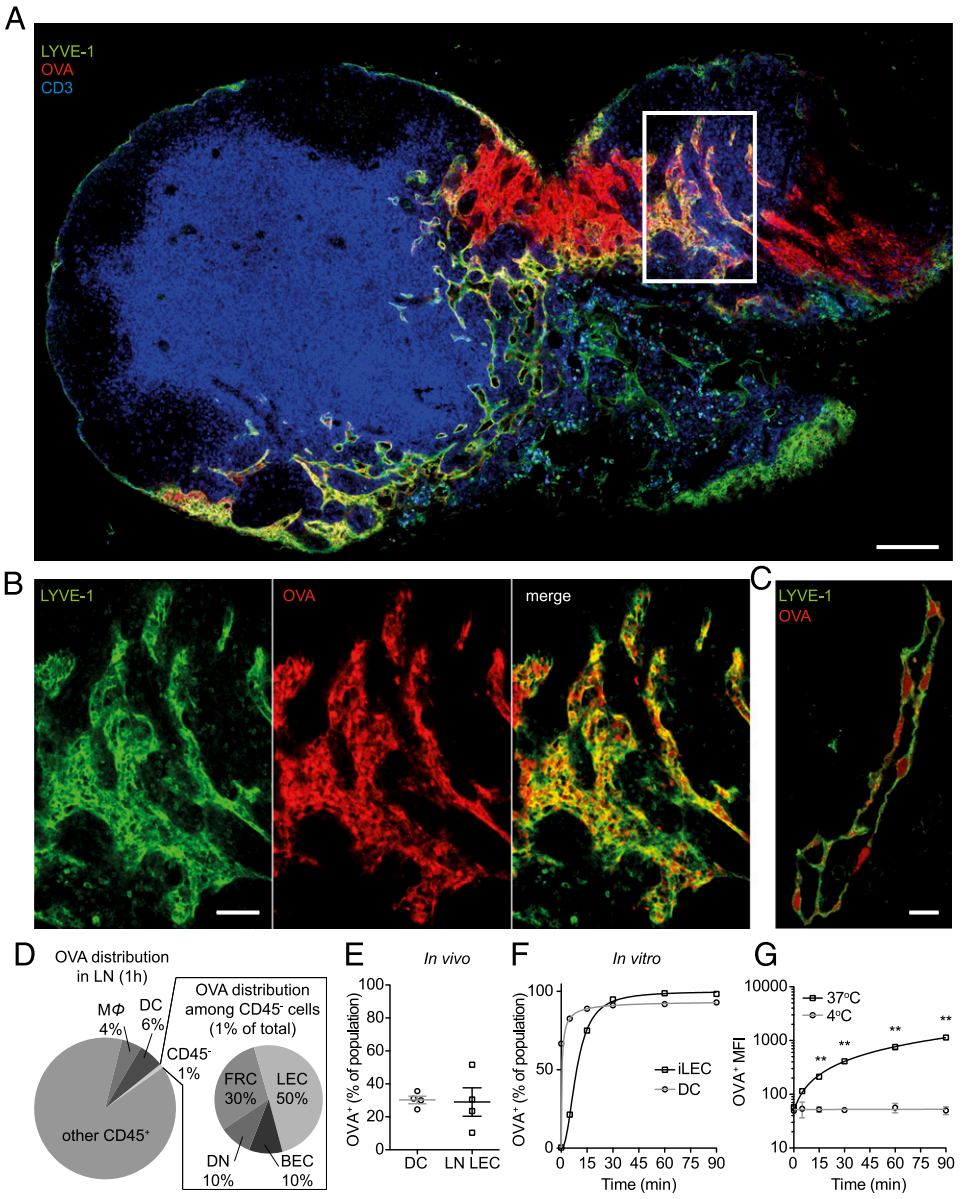

FIGURE 1. LECs scavenge exogenous protein, in vivo and in vitro. (**A**–**E**) After i.d. injection into the footpads, LECs in the draining LN take up OVA rapidly. (A) Brachial LN section showing LEC (Lyve-1, green)–associated distribution of OVA-AF647 (OVA, red) after 90 min; T cells (CD3e, blue) are shown for orientation. Scale bar, 150 μm. (B) Close-up image of region indicated by white box in (A) shows colocalization of OVA with LYVE-1$^+$ LECs. Scale bar, 75 μm. (C) LYVE-1$^+$ lymphatic vessel shows OVA$^+$ vesicles within the LECs. Scale bar, 10 μm. (D) Cellular distribution of OVA in the draining LN 90 min after i.d. injection, as analyzed by flow cytometry. Of all OVA$^+$ cells, 6% were DCs (CD11b$^{-/+}$CD11c$^+$), and 4% were macrophages (MΦ; CD11b$^+$CD11c$^-$), whereas 1% of OVA$^+$ cells in the LN were stromal cells (CD45$^-$). Among these (inset), LECs (gp38$^+$CD31$^+$) scavenged the most compared with FRCs (gp38$^+$CD31$^-$), BECs (gp38$^-$CD31$^+$), and double-negative cells (DN; gp38$^-$CD31$^-$). (E) Shown as percentages of each LN cell population positive for OVA, LECs were similar to CD11b$^-$CD11c$^+$MHCII^{mid+} DCs in their scavenging capabilities, and these two cell populations represented the highest percentage of OVA$^+$ cells among all LN cell types. Data are from two independent experiments (n = 2 each). (**F** and **G**) To demonstrate in vitro OVA accumulation, iLECs and BMDCs were incubated over 90 min at 4 or 37°C with 1 μM OVA-AF647. Cells were washed and analyzed for OVA uptake by flow cytometric analysis. (F) Percentage of OVA-AF647$^+$ cells plotted for gp38$^+$CD31$^+$-gated iLECs and CD11c$^+$-gated DCs at 37°C over time. (G) Geometric mean of OVA fluorescence is plotted for iLECs at 4°C versus 37°C. The data are representative of two independent experiments (n = 3 each). $^{**}p < 0.01$ using two-way ANOVA and Bonferroni posttest.

Because ER–golgi transport, as well as endosome acidification, was observed to be important in cross-presentation by LECs, we next asked whether exogenous Ag processing in LECs depends on the canonical TAP1 pathway, in which cytoplasmic peptide fragments are loaded onto MHC class I in the ER after translocation by TAP1 (28). Using LN LECs and DCs isolated from TAP1-null mice exposed to whole OVA protein, we found a substantial reduction in OT-I T cell proliferation after coculture compared with those exposed to LECs or DCs isolated from wild-type (WT) mice (Fig. 2D). As expected, T cell proliferation was not significantly altered between WT and TAP1-null mice with SIINFEKL stimulation, which binds externally to MHC class I, suggesting that the density of SIINFEKL/MHC class I complexes on LECs derived from both strains were comparable (Fig. 2D, Supplemental Fig. 2). Together, these data suggest that cross-presentation pathways are active in LECs.

Together, these in vitro studies establish that exogenous Ags, such as OVA and NPs, can be internalized and trafficked to in-

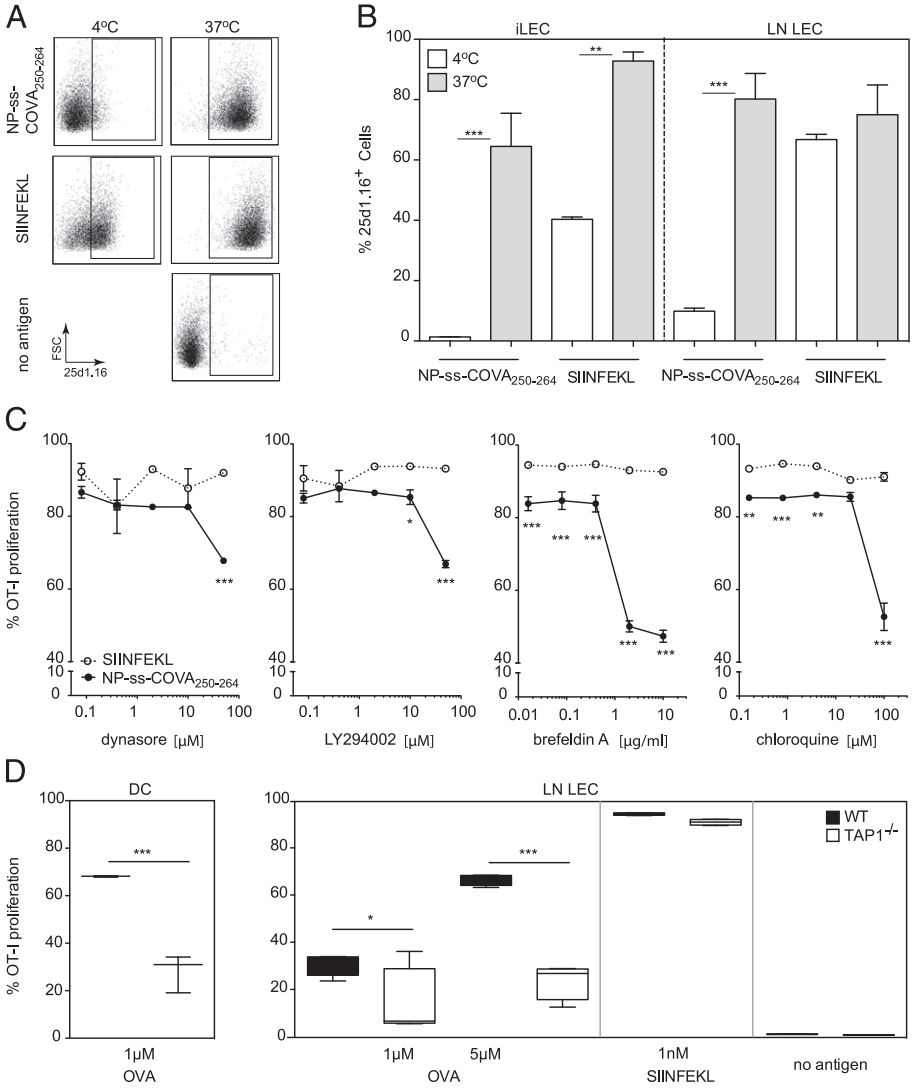

FIGURE 2. LECs process and cross-present exogenous Ag, resulting in priming naive $CD8^+$ T cells. (**A**) Detection of the MHC class I–SIINFEKL complex using the Ab 25d1.16 on ex vivo–expanded LN LECs ($CD45^-CD31^+gp38^+$) after exposure to NP-ss-$COVA_{250–264}$. Unlike the free peptide $OVA_{257–264}$ (SIINFEKL), NP-ss-$COVA_{250–264}$ cannot bind extracellularly to MHC class I; rather, the Ag must be processed intracellularly, as seen by the lack of presentation at 4˚C. (**B**) Expression of OVA peptide (SIINFEKL)–MHC class I complex by LN LECs and cultured iLECs after 18 h of incubation with NP-ss-$COVA_{250–264}$ or SIINFEKL at 2.5µ M for 18 h at 4 or 37˚C. Data shown are from two independent experiments ($n = 3$ each). (**C**) Proliferation of CFSE-labeled OT-I $CD8^+$ T cells after 3 d of coculture with iLECs is impaired in the presence of dynasore and LY294002, which block Ag uptake pathways, as well as with BFA and chloroquine, which block ER–golgi membrane trafficking and endosome acidification, respectively. A total of 1 nM SIINFEKL peptide or NP-ss-$COVA_{250–264}$ was used as Ag; the data shown are representative of two experiments ($n = 3$ each). (**D**) The ability of LECs to cross-prime OT-I $CD8^+$ T cells after OVA uptake depends on TAP1, which is required for intra-ER loading of peptides onto MHC class I molecules. Shown are percentages of proliferation of CFSE-labeled OT-I $CD8^+$ T cells after 3 d of coculture with LN LECs or DCs derived from WT or TAP1-null mice in the presence of OVA or SIINFEKL. The data shown are representative of three independent experiments ($n = 3$ each). $*p < 0.05$, $**p < 0.01$, $***p < 0.001$ using two-way ANOVA with a Bonferroni posttest.

tracellular compartments. Subsequently, LECs efficiently process Ags for cross-presentation through TAP1-dependent cytoplasmic–ER import of peptides. Both ER–golgi transport of peptide-loaded MHC class I and endosome acidification–dependent MHC class I trafficking are important for LEC cross-presentation. This suggests that some internalized Ags traffic and are loaded onto MHC class I through acidified vesicles, whereas others reach the cytosol to be imported by TAP1 for loading onto MHC class I (29).

Direct Ag-specific $CD8^+$ T cell interactions drive upregulation of MHC class I and PD-L1 on LECs

Having demonstrated the scavenger activity of LECs and efficient processing and cross-presentation of exogenous Ags, we next explored the costimulatory functions of steady-state LECs in the presence of naive $CD8^+$ T cells. We compared LEC expression of Ag-presentation molecules and costimulatory molecules with those of professional APCs (DC). As expected, DCs clearly demonstrated constitutive expression of CD40, CD86, CD80, and MHC class I that were further upregulated upon addition of the mature epitope peptide SIINFEKL and OT-I $CD8^+$ T cells (Fig. 3A, *lower panels*, OT-I and OT-I + SIINFEKL peptide, respectively). The increase in the expression levels of costimulatory molecules and receptors on the DC surface upon Ag-specific interactions with OT-I $CD8^+$ T cells might appear surprising in the absence of TLR stimulation. However, TLR-independent pathways exist that can drive maturation, and it was reported that cognate interactions between DCs and $CD8^+$ T cells alone can induce upregulation of CD80 and CD86 expression on DCs (30).

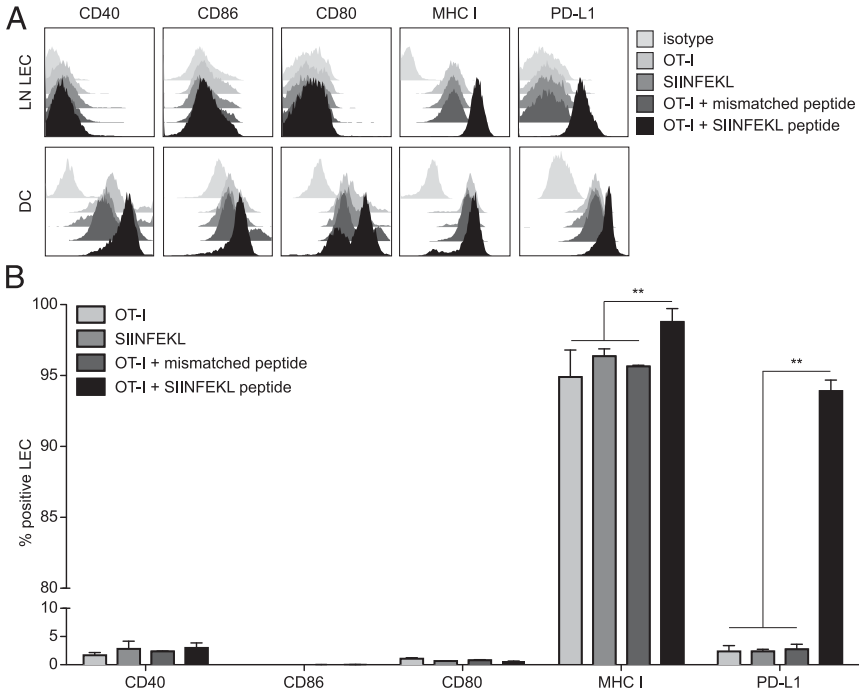

FIGURE 3. Ag-specific interaction with naive CD8$^+$ T cells results in upregulation of MHC class I and PD-L1 expression on LECs. (**A** and **B**) In the presence of Ag-specific CD8$^+$ T cells in vitro, the LEC phenotype suggests coinhibitory signaling. Naive OVA-specific OT-I CD8$^+$ T cells were cocultured with ex vivo–expanded LN LECs or BMDCs from C57BL/6 mice in the presence (OT-I + SIINFEKL peptide) or absence (OT-I) of 1 nM SIINFEKL, the immunodominant MHC class I peptide of OVA, or 1 nM AMQMLKETI peptide (OT-I + mismatched peptide). As an additional control, DCs or LN LECs also were incubated with 1 nM SIINFEKL in the absence of CD8$^+$ T cells (SIINFEKL). After 24 h of T cell/LEC or T cell/DC coculture, the relative expression levels of costimulatory molecules CD40, CD86 (B7-2), CD80 (B7-1), MHC class I, and PD-L1 (or B7-H1) were determined by flow cytometric analysis. (A) Representative graphs for each marker are shown on gp38$^+$CD31$^+$-gated LN LECs or CD11c$^+$-gated DCs incubated with OT-I + SIINFEKL, OT-I + mismatched peptide, SIINFEKL only, OT-I only, or isotype control. (B) Percentages of CD40$^+$, CD86$^+$, CD80$^+$, MHC class I$^+$, and PD-L1$^+$ cells in gp38$^+$CD31$^+$-gated LN LECs in each case. Data are mean ± SD from one of two representative experiments (n = 3 each). $^{**}p < 0.01$ using two-way ANOVA followed by Bonferroni posttest.

Furthermore, the transport of peptide-loaded MHC class I to the cell surface was suggested to be accompanied by an increased expression of costimulatory molecules (31). Thus, peptide loading of MHC class I and subsequent engagement of TCR and T cell activation can indirectly upregulate costimulatory molecules on DCs. Because our peptide was not contaminated with endotoxin, and the observed changes in maturation markers were not induced when DCs were incubated with the cognate peptide in the absence of CD8$^+$ T cells (Fig. 3A, *lower panels*, SIINFEKL), our data suggest that Ag presentation by the APC and subsequent recognition by the T cell leads to the altered expression. In contrast to expression by DCs, ex vivo–cultured primary LN LECs expressed low levels of CD40 and CD80 and undetectable levels of CD86 in either the presence or absence of Ag-specific interactions with CD8$^+$ T cells (Fig. 3A, *upper panels*). Similarly, constitutive expression of costimulatory molecules in human LECs was lower than that of human blood-derived DCs (data not shown). However, LECs significantly upregulated MHC class I ($p < 0.01$) in a manner that was dependent on Ag-specific CD8$^+$ T cell interactions (Fig. 3).

Consistent with previous reports (32, 33), both LECs and DCs constitutively expressed the inhibitory ligand PD-L1 (or B7.H-1, Fig. 3A), which was reported to attenuate T cell proliferation and abrogate effector T cell differentiation (34). Furthermore, both LECs and DCs expressed higher levels of cell surface PD-L1 upon cognate interactions with CD8$^+$ T cells (Fig. 3A, OT-I + SIINFEKL peptide). Although DCs expressed higher baseline levels of PD-L1 compared with LECs, the upregulation of PD-L1 upon cognate Ag-specific CD8$^+$ T cell interaction was much more pronounced in LECs than in DCs (Fig. 3, Supplemental Fig. 3). More importantly, this change was not accompanied by increased costimulatory molecule expression in LECs, as it clearly was in DCs. The same trends also were observed in cultured iLECs (data not shown). Collectively, these data demonstrate an evidently different balance between costimulatory and coinhibitory ligand expression in LECs versus DCs and further suggest that Ag-specific interactions between LECs and CD8$^+$ T cells result in dynamic regulation of the LEC phenotype to favor coinhibitory signaling.

Cross-presentation of exogenous Ag by LECs leads to impaired activation of naive CD8$^+$ T cells in an Ag-specific manner

Having shown that Ag-presenting LECs can upregulate PD-L1 in the presence of Ag-specific CD8$^+$ T cells in vitro, we next asked whether cross-presentation by LECs and engagement of Ag-specific TCRs could lead to a tolerized phenotype of CD8$^+$ T cells under steady-state conditions. To this end, we investigated the functional capacity of CD8$^+$ T cells after cross-priming by LECs compared with cross-priming by DCs in vitro. Upon incubation with iLECs in the presence of 1 nM NP-ss-COVA$_{250–264}$, OT-I CD8$^+$ T cells proliferated strongly; however, these iLEC-primed CD8$^+$ T cells displayed a dysfunctionally activated phenotype characterized by high levels of the apoptotic marker annexin V in early generations of proliferating T cells compared with DC-stimulated T cells (Fig. 4A).

The upregulation of PD-L1 on LECs upon Ag-specific interactions with CD8$^+$ T cells (Fig. 3) led us to analyze the expression of PD-L1–binding partners PD-1 and CD80 on cocultured CD8$^+$ T cells. PD-1 is a member of the B7/CD28 superfamily and plays

a central role in the regulation of T cell immunity; its activation results in decreased proliferation, reduced IFN-γ and IL-2 production, and increased apoptosis (34). We observed that PD-1 expression was consistently high on iLEC-stimulated $CD8^+$ T cells from the early proliferative generations, whereas only later generations of DC-stimulated $CD8^+$ T cells expressed elevated levels of PD-1 (Fig. 4A). In addition to PD-1, recent studies showed that PD-L1 binds CD80 at a distinct site (35) to deliver inhibitory signals to T cells (36); in those studies, CD80 expression was observed on anergic T cells and was further upregulated after re-exposure to the Ag. In contrast to DC-stimulated $CD8^+$ T cells, we detected a high percentage of CD80 expression on proliferating iLEC-primed $CD8^+$ T cells (Fig. 4A). In addition to PD-1, CTLA-4 was substantially upregulated in early generations of $CD8^+$ T cells stimulated by LECs versus DCs (Fig. 4A). CTLA-4 is another member of the CD28/B7 superfamily, which is implicated in tolerogenic responses with a distinct, nonredundant regulatory role (34, 37), and competes with CD28 for binding to CD80 and CD86 on APCs to impede costimulatory signaling and increase CD86 degradation, resulting in impaired T cell activation (38). CTLA-4 also disrupts positive signaling through recruitment of phosphatases to the immunological synapse and subsequent dephosphorylation of key signaling molecules without direct engagement to CD80 and CD86 (38). In addition to CTLA-4 upregulation, we found reduced expression of the surface activation markers CD25, CD44, and CD69 in iLEC-primed T cells compared with DC-primed T cells (Fig. 4B). Finally, OT-I $CD8^+$ T cells primed with iLECs in the presence of NP-ss-$COVA_{250–264}$ produced significantly less IFN-γ and IL-2 compared with T cells primed with DCs (Fig. 4C).

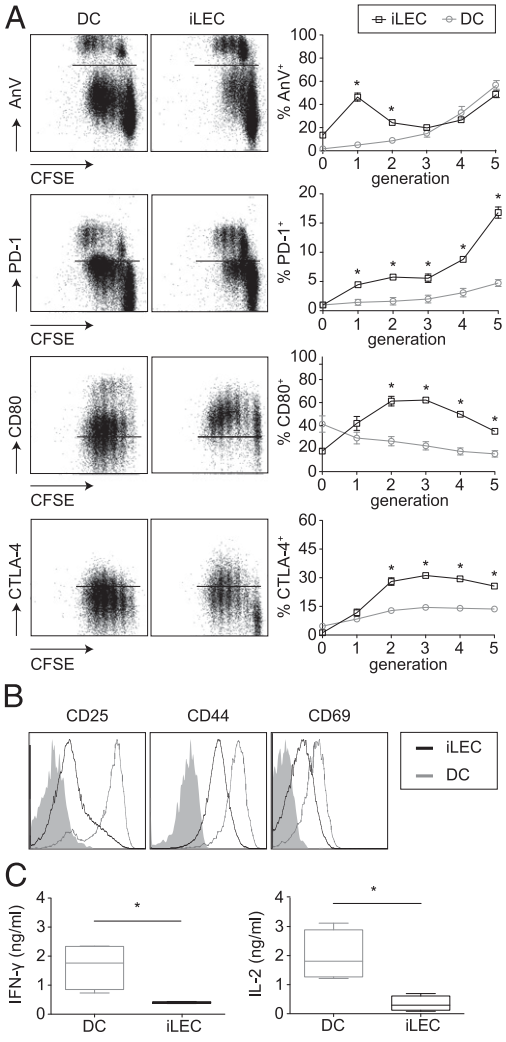

FIGURE 4. Cross-presentation by LECs induces impaired $CD8^+$ T cell proliferation. Naive CFSE-labeled OVA-specific OT-I $CD8^+$ T cells were cocultured with iLECs or BMDCs from C57BL/6 mice in the presence of NP-ss-$COVA_{250–264}$ at 1 nM and analyzed after 3 d. (**A**) Phenotypes of OT-I $CD8^+$ T cells after priming by cross-presenting DCs or iLECs, as analyzed by flow cytometric evaluation of annexin V, PD-1, CD80 (B7-1), and CTLA-4 surface marker expression. Representative dot plots from live-gated cells (*left panels*). Percentages of positive cells/generation from one representative of three to five independent experiments (n = 3–4 each) (*right panels*). (**B**) Representative flow cytometry graphs showing activation marker expression on OT-I $CD8^+$ cells after 3 d of cross-priming by iLECs or DCs; shaded graphs show naive (noneducated) OT-I $CD8^+$ T cells. (**C**) Cytokine secretion by iLEC- or DC-educated OT-I $CD8^+$ T cells, as assessed by ELISA. Data are mean ± SD from one representative experiment of four (n = 4 each). *$p < 0.05$ using two-way ANOVA followed by Bonferroni posttest.

Taken together, these data indicate that iLECs can efficiently cross-present Ag and directly interact with $CD8^+$ T cells to induce Ag-specific proliferating T cells with a tolerized phenotype in vitro. The functional outcome of T cell priming differs significantly from that of T cells primed by conventional APCs, suggesting a tolerizing role for LECs under steady-state conditions.

IL-2 does not rescue the dysfunctional phenotype of $CD8^+$ T cells activated by LECs

Because we observed diminished levels of IL-2 production by LEC-stimulated versus DC-stimulated T cells (Fig. 4C), and because IL-2 is essential for $CD8^+$ T cell expansion, we asked whether the T cell phenotype could be rescued by exogenous IL-2, as was shown for exhausted T cells in chronic viral infection (39). Interestingly, supplementation of the iLEC–T cell cocultures with IL-2 (50 U/ml) resulted in increased expression of the activation markers CD25, CD44, and CD69 on $CD8^+$ T cells (Fig. 5A). However, no effect was seen on T cell proliferation or IFN-γ production (Fig. 5B), nor did IL-2 significantly decrease the percentages of annexin V^+ or PD-1^+ cells per generation (Fig. 5C). These trends were similar when LN LECs were treated with NP-ss-$COVA_{250–264}$ and when iLECs were stimulated with 1 μM OVA protein instead of NP-ss-$COVA_{250–264}$ (data not shown). Together, these data suggest that $CD8^+$ T cells cross-primed by LECs were not merely exhausted, because they could not be rescued by IL-2.

Discussion

In addition to carrying Ags to the LN for uptake by immature DCs for immune surveillance, this study highlights an important role for lymphatic drainage in the maintenance of peripheral tolerance: the constant exposure of LECs to lymph-borne peripheral Ags, which they scavenge and cross-present for tolerance induction under steady-state conditions. Ag cross-presentation was dependent on ER–golgi trafficking, endosome acidification, and TAP1. We observed that Ag-specific interactions with $CD8^+$ T cells resulted in upregulation of MHC class I and PD-L1 on LECs and dysfunctional activation of $CD8^+$ T cells, which displayed early apoptosis and diminished cytokine production. Thus, in addition to the previously described role of LECs in presenting endogenous PTAs for autoreactive $CD8^+$ T cell deletion (6–8), the current study demonstrates that LECs can efficiently scavenge and cross-present foreign Ags draining from the periphery; thus, they play an immunoprotective role against a broader range of peripheral Ags.

Until recently, the cross-presentation mechanism in the induction of peripheral tolerance to exogenous Ags by nonhematopoietic stromal cells has been almost exclusively attributed to LSECs,

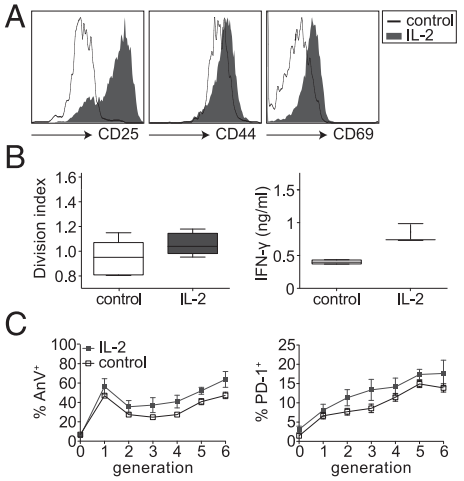

FIGURE 5. The LEC-educated T cell phenotype is only partially reversed by IL-2. Naive CFSE-labeled OVA-specific OT-I $CD8^+$ T cells were cocultured with iLECs for 3 d in the presence of Ag (1 nM NP-ss-$COVA_{250–264}$) and supplemented with 50 U/ml IL-2. (**A**) Representative flow cytometry graphs showing OT-I surface expression of activation markers after 3 d of priming by iLECs in the absence or presence of IL-2. Data are representative of three independent experiments ($n = 4$ each). (**B**) Division index of proliferating OT-I $CD8^+$ T cells (*left panel*) and IFN-γ release (*right panel*) were affected only slightly by IL-2. Data are mean ± SD from one representative of four independent experiments ($n = 4$ each). (**C**) Percentages of annexin V^+ and PD-1^+ OT-I $CD8^+$ T cells/generation after 3 d of coculture with iLECs are unaffected by IL-2. Data are mean ± SD from two independent experiments ($n = 7$ each).

which line the hepatic sinusoidal wall and come into close contact with foreign Ags and leukocytes passing through the liver (40). Similarly, LECs are positioned in a strategic anatomical site where crucial interactions determining the fate of an immune response take place. In this study, we demonstrated that Ag scavenging by LECs occurs under noninflammatory steady-state conditions, adding to our previous observation that tumor-associated LECs cross-present OVA expressed by B16-F10 tumors (16). Murine LECs in the skin-draining LNs actively took up peripherally administered OVA protein under steady-state conditions (Fig. 1A–C), consistent with an earlier study (41), and could be mediated through LEC expression of the mannose receptor (42, 43). This was further supported by our data showing that LN LECs were as effective as DCs in taking up OVA (Fig. 1E, Supplemental Fig. 1). This is consistent with continual scavenging of inflammatory CC chemokines (44) by D6 on afferent and subcapsular LECs, which results in intracellular degradation and reduction in the inflammatory chemokines entering the LNs under homeostatic conditions (45). Together with the data presented in this article, we conclude that LECs constitutively scavenge molecules to sample the peripheral lymph entering the LNs.

We turned to in vitro studies to characterize the details of exogenous Ag cross-presenting mechanisms in LECs and found strong dependencies on temperature, dynamin-mediated uptake, intracellular Ag transporters, and TAP1 (Fig. 2), implicating similar cross-presentation pathways as those seen in DCs. Specifically, inhibitor sensitivity data suggested that both dynamin (clathrin/caveolin) and PI3K (phagocytosis/macropinocytosis) pathways contribute to cross-presentation and T cell priming by LECs (Fig. 2C). This is in agreement with confocal microscopy studies (Supplemental Fig. 4) showing OVA colocalization with the clathrin H chain in LECs at early times after exposure. Similar observations were made with LSECs (14) and are consistent with early endosome colocalization observed in BMDCs (46). At later time points, OVA was found in LAMP-1^+ vesicles, supporting the data showing chloroquine inhibition of Ag cross-presentation (Supplemental Fig. 4).

A hallmark of cross-presentation of exogenous Ags by professional APCs is the dependence on TAP1 (47). As described for other murine stromal cells, such as LSECs (14, 48), aortic endothelial cells (49), and thymic stromal cells (50), we found that the TAP1-dependent transport of cytoplasmic peptides into the ER (Fig. 2D) and ER–golgi trafficking (Fig. 2C) were important in Ag-specific $CD8^+$ T cell proliferation upon LEC cross-presentation. Furthermore, our data indicate that TAP1-independent pathways also may be active in LECs (Fig. 2D). In APCs, more than one pathway for loading of mature peptide epitopes on MHC class I have been described, including loading in phagolysosomes or recycling endosomes (29, 51, 52). Intraphagosome or lysosome release and MHC class I loading of peptides in LAMP-$1^+$$MHCI^+$ compartments were described for DCs (53), which would be consistent with the chloroquine sensitivity observed (Fig. 2C) and Ag presence in LAMP-1^+ vesicles in LECs (Supplemental Fig. 4).

Although LECs displayed several similarities to LSECs with regard to Ag processing and cross-presenting capacity, LECs displayed some phenotypic differences to LSECs. For example, under steady-state conditions, LSECs were shown to express the costimulatory molecules CD40, CD80, and CD86 (30), LECs lack an immunostimulatory phenotype with remarkably low expression of costimulatory molecules (Fig. 3). Because the endotoxin levels found in portal blood under physiological conditions are presumably higher than in peripheral lymph, it is not surprising that the steady-state set point of costimulatory molecules in LSECs is higher than in LECs. The inability of LECs to upregulate the costimulation machinery, together with PD-L1 upregulation upon Ag-specific T cell interactions (Fig. 3, Supplemental Fig. 3), suggest that LEC cross-presentation may be nonactivating, because lack of costimulation is one mechanism of a dysfunctional $CD8^+$ T cell response that is reminiscent of the classical mechanism of peripheral tolerance induction by immature DCs under noninflammatory conditions by T cell anergy and deletion (54).

The functional discrepancy and fate of LEC-primed versus DC-primed $CD8^+$ T cells (Fig. 4C) was coupled with the reciprocal upregulation of inhibitory molecular partners on $CD8^+$ T cells: the PD-L1 partners PD-1 and CD80, as well as CTLA-4 (Fig. 4A). In accordance with our observations, Tewalt et al. (6) recently demonstrated a key role for the PD-L1/PD-1–signaling pathway in the absence of costimulation in LEC-induced peripheral tolerance of endogenously expressed PTAs, where blocking PD-1 in LEC-educated, tyrosinase-specific $CD8^+$ T cells resulted in autoimmune vitiligo. Although exogenous IL-2 compensated for PD-L1–mediated coinhibitory signaling in the absence of costimulatory molecules in LSEC–T cell cocultures (55), supplementation of LEC–T cell cocultures with IL-2 did not alter the phenotype of LEC-primed $CD8^+$ T cells (Fig. 5). Our data suggest that other regulatory pathways might be involved, such as the engagement of PD-L1 by CD80 or signaling through CTLA-4, or additional ligands that are reported to be expressed on LEC surface, including the B and T lymphocyte attenuator molecule or the lymphocyte activation gene 3 (6). Interestingly, there may be more than one differentiation state of $CD8^+$ T cells; apparently tolerized LSEC cross-primed $CD8^+$ T cells (30), upon inflammatory recall, were capable of becoming effector cells, reminiscent of central memory T cell activity (56). This may also apply in steady-state LEC cross-primed $CD8^+$ T cells. Further detailed mechanistic studies must be conducted on the coordination (57) of Ag processing, presentation, and costimulatory/coinhibitory molecule pathways to shape the fate of these cells.

Because LECs are situated in one of the prime anatomical sites for immunological sampling, our findings support the idea that organ-draining LECs are the first to sample and present the exogenous peptides (3, 58), proteins, and particulates present in lymph. Thus, LECs may play an important role in the context of immunomodulation. Several findings from the literature support this concept that flow from the periphery and the presence of lymphatics are important in shaping the adaptive immune responses in the LN. For example, Friedlaender and Baer (59) showed in 1972 that skin missing lymphatic connections was more readily sensitized to dansyl chloride than was intact skin, suggesting that the presence of lymphatics in intact skin contributes to a dampened delayed-type hypersensitivity response. Using the K14–VEGFR-3–Ig mice model, we previously showed how impaired lymph drainage and the absence of dermal LECs resulted in impaired acquired tolerance to contact hypersensitivity, although these mice could mount a systemic T cell response (60). In the experimental autoimmune encephalomyelitis model, impaired lymphatic contraction and fluid drainage were reported to result in an autoimmune response (61). Together, this suggests that impaired lymphatic drainage translates to an inappropriately activated immune response. Reciprocally, steady-state drainage of Ag to LN seems to favor tolerogenic responses. For example, the clinical success of allergen-specific immune therapy is based on a regimen of long-term s.c. low-dose allergen injection (62). We showed that VEGF-C–expanded tumor-draining LN LECs impede a robust Ag-specific $CD8^+$ T cell response, which promotes tumor growth (16). In keeping with the idea that peripheral tolerance requires persistent Ag (63), continuous access to draining peripheral Ags newly establishes LECs as active players in the maintenance of a tolerogenic LN environment. It implies that, after injury or infection, when self-Ags drain to the LN, together with TLRs and other danger signals, the steady-state tolerization by LECs can act as a dampening mechanism to prevent later potential autoimmune reactions. In other words, LEC cross-presentation of draining Ags helps to amplify the signal-to-noise ratio between dangerous Ags and those that have been encountered under steady-state conditions.

This work demonstrates that priming by LECs, via direct cross-presentation of scavenged exogenous Ags, has a tolerizing effect on $CD8^+$ T cells. In addition to T cell tolerization against LEC-expressed PTAs (6–8) and contact-dependent immunosuppression of APCs (11), we establish LECs as bona fide APCs that are capable of sampling the peripheral Ag repertoire by active internalization and cross-presentation of Ags on MHC I molecules. This steady-state cross-presentation of scavenged peripheral Ags by LECs highlights the importance of lymphatic drainage and the role of LECs in immunomodulation, which may contribute an additional layer of control against self-reactive T cells in the context of maintaining self-tolerance against draining peripheral Ags during homeostasis or tissue injury. These findings help to explain why tumor-associated lymphatics promote tumor progression and metastasis to distant sites and why dysfunctional lymphatic drainage is correlated with autoimmunity.

Acknowledgments

We thank Fernanda Duraes, Juan Dubrot Armendariz, Anna Mondino, Catherine Card, Edward Phelps, and Ingrid van Mier for helpful discussions.

Disclosures

The authors have no financial conflicts of interest.

References

1. Oliver, G., and K. Alitalo. 2005. The lymphatic vasculature: recent progress and paradigms. *Annu. Rev. Cell Dev. Biol.* 21: 457–483.
2. Tal, O., H. Y. Lim, I. Gurevich, I. Milo, Z. Shipony, L. G. Ng, V. Angeli, and G. Shakhar. 2011. DC mobilization from the skin requires docking to immobilized CCL21 on lymphatic endothelium and intralymphatic crawling. *J. Exp. Med.* 208: 2141–2153.
3. Clement, C. C., E. S. Cannizzo, M.-D. Nastke, R. Sahu, W. Olszewski, N. E. Miller, L. J. Stern, and L. Santambrogio. 2010. An expanded self-antigen peptidome is carried by the human lymph as compared to the plasma. *PLoS ONE* 5: e9863.
4. Fletcher, A. L., D. Malhotra, and S. J. Turley. 2011. Lymph node stroma broaden the peripheral tolerance paradigm. *Trends Immunol.* 32: 12–18.
5. Graham, G. J. 2009. D6 and the atypical chemokine receptor family: novel regulators of immune and inflammatory processes. *Eur. J. Immunol.* 39: 342–351.
6. Tewalt, E. F., J. N. Cohen, S. J. Rouhani, C. J. Guidi, H. Qiao, S. P. Fahl, M. R. Conaway, T. P. Bender, K. S. Tung, A. T. Vella, et al. 2012. Lymphatic endothelial cells induce tolerance via PD-L1 and lack of costimulation leading to high-level PD-1 expression on CD8 T cells. *Blood* 120: 4772–4782.
7. Cohen, J. N., C. J. Guidi, E. F. Tewalt, H. Qiao, S. J. Rouhani, A. Ruddell, A. G. Farr, K. S. Tung, and V. H. Engelhard. 2010. Lymph node-resident lymphatic endothelial cells mediate peripheral tolerance via Aire-independent direct antigen presentation. *J. Exp. Med.* 207: 681–688.
8. Fletcher, A. L., V. Lukacs-Kornek, E. D. Reynoso, S. E. Pinner, A. Bellemare-Pelletier, M. S. Curry, A. R. Collier, R. L. Boyd, and S. J. Turley. 2010. Lymph node fibroblastic reticular cells directly present peripheral tissue antigen under steady-state and inflammatory conditions. *J. Exp. Med.* 207: 689–697.
9. Lukacs-Kornek, V., D. Malhotra, A. L. Fletcher, S. E. Acton, K. G. Elpek, P. Tayalia, A.-R. Collier, and S. J. Turley. 2011. Regulated release of nitric oxide by nonhematopoietic stroma controls expansion of the activated T cell pool in lymph nodes. *Nat. Immunol.* 12: 1096–1104.
10. Swartz, M. A., and A. W. Lund. 2012. Lymphatic and interstitial flow in the tumour microenvironment: linking mechanobiology with immunity. *Nat. Rev. Cancer* 12: 210–219.
11. Podgrabinska, S., O. Kamalu, L. Mayer, M. Shimaoka, H. Snoeck, G. J. Randolph, and M. Skobe. 2009. Inflamed lymphatic endothelium suppresses dendritic cell maturation and function via Mac-1/ICAM-1-dependent mechanism. *J. Immunol.* 183: 1767–1779.
12. Nörder, M., M. G. Gutierrez, S. Zicari, E. Cervi, A. Caruso, and C. A. Guzmán. 2012. Lymph node-derived lymphatic endothelial cells express functional costimulatory molecules and impair dendritic cell-induced allogenic T-cell proliferation. *FASEB J.* 26: 2835–2846.
13. Reynoso, E. D., and S. J. Turley. 2009. Unconventional antigen-presenting cells in the induction of peripheral CD8(+) T cell tolerance. *J. Leukoc. Biol.* 86: 795–801.
14. Schurich, A., J. P. Böttcher, S. Burgdorf, P. Penzler, S. Hegenbarth, M. Kern, A. Dolf, E. Endl, J. Schultze, E. Wiertz, et al. 2009. Distinct kinetics and dynamics of cross-presentation in liver sinusoidal endothelial cells compared to dendritic cells. *Hepatology* 50: 909–919.
15. von Oppen, N., A. Schurich, S. Hegenbarth, D. Stabenow, R. Tolba, R. Weiskirchen, A. Geerts, W. Kolanus, P. Knolle, and L. Diehl. 2009. Systemic antigen cross-presented by liver sinusoidal endothelial cells induces liver-specific CD8 T-cell retention and tolerization. *Hepatology* 49: 1664–1672.
16. Lund, A. W., F. V. Duraes, S. Hirosue, V. R. Raghavan, C. Nembrini, S. N. Thomas, A. Issa, S. Hugues, and M. A. Swartz. 2012. VEGF-C promotes immune tolerance in B16 melanomas and cross-presentation of tumor antigen by lymph node lymphatics. *Cell. Rep.* 1: 191–199.
17. Shields, J. D., I. C. Kourtis, A. A. Tomei, J. M. Roberts, and M. A. Swartz. 2010. Induction of lymphoidlike stroma and immune escape by tumors that express the chemokine CCL21. *Science* 328: 749–752.
18. Jat, P. S., M. D. Noble, P. Ataliotis, Y. Tanaka, N. Yannoutsos, L. Larsen, and D. Kioussis. 1991. Direct derivation of conditionally immortal cell lines from an H-2Kb-tsA58 transgenic mouse. *Proc. Natl. Acad. Sci. USA* 88: 5096–5100.
19. Fletcher, A. L., D. Malhotra, S. E. Acton, V. Lukacs-Kornek, A. Bellemare-Pelletier, M. Curry, M. Armant, and S. J. Turley. 2011. Reproducible isolation of lymph node stromal cells reveals site-dependent differences in fibroblastic reticular cells. *Front. Immunol.* 2: 35.
20. Link, A., T. K. Vogt, S. Favre, M. R. Britschgi, H. Acha-Orbea, B. Hinz, J. G. Cyster, and S. A. Luther. 2007. Fibroblastic reticular cells in lymph nodes regulate the homeostasis of naive T cells. *Nat. Immunol.* 8: 1255–1265.
21. Lutz, M. B., N. Kukutsch, A. L. Ogilvie, S. Rössner, F. Koch, N. Romani, and G. Schuler. 1999. An advanced culture method for generating large quantities of highly pure dendritic cells from mouse bone marrow. *J. Immunol. Methods* 223: 77–92.
22. Hirosue, S., I. C. Kourtis, A. J. van der Vlies, J. A. Hubbell, and M. A. Swartz. 2010. Antigen delivery to dendritic cells by poly(propylene sulfide) nanoparticles with disulfide conjugated peptides: Cross-presentation and T cell activation. *Vaccine* 28: 7897–7906.
23. Fletcher, P. A., D. R. Scriven, M. N. Schulson, and E. D. Moore. 2010. Multi-image colocalization and its statistical significance. *Biophys. J.* 99: 1996–2005.
24. Macia, E., M. Ehrlich, R. Massol, E. Boucrot, C. Brunner, and T. Kirchhausen. 2006. Dynasore, a cell-permeable inhibitor of dynamin. *Dev. Cell* 10: 839–850.
25. Araki, N., M. T. Johnson, and J. A. Swanson. 1996. A role for phosphoinositide 3-kinase in the completion of macropinocytosis and phagocytosis by macrophages. *J. Cell Biol.* 135: 1249–1260.
26. Fujiwara, T., K. Oda, S. Yokota, A. Takatsuki, and Y. Ikehara. 1988. Brefeldin A causes disassembly of the Golgi complex and accumulation of secretory proteins in the endoplasmic reticulum. *J. Biol. Chem.* 263: 18545–18552.
27. Steinman, R. M., I. S. Mellman, W. A. Muller, and Z. A. Cohn. 1983. Endocytosis and the recycling of plasma membrane. *J. Cell Biol.* 96: 1–27.
28. Brossart, P., and M. J. Bevan. 1997. Presentation of exogenous protein antigens on major histocompatibility complex class I molecules by dendritic cells: pathway of presentation and regulation by cytokines. *Blood* 90: 1594–1599.

29. Grommé, M., F. G. Uytdehaag, H. Janssen, J. Calafat, R. S. van Binnendijk, M. J. Kenter, A. Tulp, D. Verwoerd, and J. Neefjes. 1999. Recycling MHC class I molecules and endosomal peptide loading. *Proc. Natl. Acad. Sci. USA* 96: 10326–10331.
30. Diehl, L., A. Schurich, R. Grochtmann, S. Hegenbarth, L. Chen, and P. A. Knolle. 2008. Tolerogenic maturation of liver sinusoidal endothelial cells promotes B7-homolog 1-dependent CD8+ T cell tolerance. *Hepatology* 47: 296–305.
31. Schmidt, S. V., A. C. Nino-Castro, and J. L. Schultze. 2012. Regulatory dendritic cells: there is more than just immune activation. *Front. Immunol.* 3: 274.
32. Freeman, G. J., A. J. Long, Y. Iwai, K. Bourque, T. Chernova, H. Nishimura, L. J. Fitz, N. Malenkovich, T. Okazaki, M. C. Byrne, et al. 2000. Engagement of the PD-1 immunoinhibitory receptor by a novel B7 family member leads to negative regulation of lymphocyte activation. *J. Exp. Med.* 192: 1027–1034.
33. Keir, M. E., M. J. Butte, G. J. Freeman, and A. H. Sharpe. 2008. PD-1 and its ligands in tolerance and immunity. *Annu. Rev. Immunol.* 26: 677–704.
34. McGrath, M. M., and N. Najafian. 2012. The role of coinhibitory signaling pathways in transplantation and tolerance. *Front. Immunol.* 3: 47.
35. Butte, M. J., M. E. Keir, T. B. Phamduy, A. H. Sharpe, and G. J. Freeman. 2007. Programmed death-1 ligand 1 interacts specifically with the B7-1 costimulatory molecule to inhibit T cell responses. *Immunity* 27: 111–122.
36. Park, J.-J., R. Omiya, Y. Matsumura, Y. Sakoda, A. Kuramasu, M. M. Augustine, S. Yao, F. Tsushima, H. Narazaki, S. Anand, et al. 2010. B7-H1/CD80 interaction is required for the induction and maintenance of peripheral T-cell tolerance. *Blood* 116: 1291–1298.
37. Chen, L., and D. B. Flies. 2013. Molecular mechanisms of T cell co-stimulation and co-inhibition. *Nat. Rev. Immunol.* 13: 227–242.
38. Rudd, C. E., A. Taylor, and H. Schneider. 2009. CD28 and CTLA-4 coreceptor expression and signal transduction. *Immunol. Rev.* 229: 12–26.
39. Blattman, J. N., J. M. Grayson, E. J. Wherry, S. M. Kaech, K. A. Smith, and R. Ahmed. 2003. Therapeutic use of IL-2 to enhance antiviral T-cell responses in vivo. *Nat. Med.* 9: 540–547.
40. Crispe, I. N. 2003. Hepatic T cells and liver tolerance. *Nat. Rev. Immunol.* 3: 51–62.
41. Sixt, M., N. Kanazawa, M. Selg, T. Samson, G. Roos, D. P. Reinhardt, R. Pabst, M. B. Lutz, and L. Sorokin. 2005. The conduit system transports soluble antigens from the afferent lymph to resident dendritic cells in the T cell area of the lymph node. *Immunity* 22: 19–29.
42. Irjala, H., K. Alanen, R. Grénman, P. Heikkilä, H. Joensuu, and S. Jalkanen. 2003. Mannose receptor (MR) and common lymphatic endothelial and vascular endothelial receptor (CLEVER)-1 direct the binding of cancer cells to the lymph vessel endothelium. *Cancer Res.* 63: 4671–4676.
43. Marttila-Ichihara, F., R. Turja, M. Miiluniemi, M. Karikoski, M. Maksimow, J. Niemelä, L. Martinez-Pomares, M. Salmi, and S. Jalkanen. 2008. Macrophage mannose receptor on lymphatics controls cell trafficking. *Blood* 112: 64–72.
44. Lee, K. M., R. J. Nibbs, and G. J. Graham. 2013. D6: the 'crowd controller' at the immune gateway. *Trends Immunol.* 34: 7–12.
45. Nibbs, R. J., P. McLean, C. McCulloch, A. Riboldi-Tunnicliffe, E. Blair, Y. Zhu, N. Isaacs, and G. J. Graham. 2009. Structure-function dissection of D6, an atypical scavenger receptor. *Methods Enzymol.* 460: 245–261.
46. Burgdorf, S., A. Kautz, V. Böhnert, P. A. Knolle, and C. Kurts. 2007. Distinct pathways of antigen uptake and intracellular routing in CD4 and CD8 T cell activation. *Science* 316: 612–616.
47. Joffre, O. P., E. Segura, A. Savina, and S. Amigorena. 2012. Cross-presentation by dendritic cells. *Nat. Rev. Immunol.* 12: 557–569.
48. Limmer, A., J. Ohl, C. Kurts, H. G. Ljunggren, Y. Reiss, M. Groettrup, F. Momburg, B. Arnold, and P. A. Knolle. 2000. Efficient presentation of exogenous antigen by liver endothelial cells to CD8+ T cells results in antigen-specific T-cell tolerance. *Nat. Med.* 6: 1348–1354.
49. Bagai, R., A. Valujskikh, D. H. Canaday, E. Bailey, P. N. Lalli, C. V. Harding, and P. S. Heeger. 2005. Mouse endothelial cells cross-present lymphocyte-derived antigen on class I MHC via a TAP1- and proteasome-dependent pathway. *J. Immunol.* 174: 7711–7715.
50. Merkenschlager, M., M. O. Power, H. Pircher, and A. G. Fisher. 1999. Intrathymic deletion of MHC class I-restricted cytotoxic T cell precursors by constitutive cross-presentation of exogenous antigen. *Eur. J. Immunol.* 29: 1477–1486.
51. Guermonprez, P., L. Saveanu, M. Kleijmeer, J. Davoust, P. Van Endert, and S. Amigorena. 2003. ER-phagosome fusion defines an MHC class I cross-presentation compartment in dendritic cells. *Nature* 425: 397–402.
52. Houde, M., S. Bertholet, E. Gagnon, S. Brunet, G. Goyette, A. Laplante, M. F. Princiotta, P. Thibault, D. Sacks, and M. Desjardins. 2003. Phagosomes are competent organelles for antigen cross-presentation. *Nature* 425: 402–406.
53. Lizée, G., G. Basha, J. Tiong, J.-P. Julien, M. Tian, K. E. Biron, and W. A. Jefferies. 2003. Control of dendritic cell cross-presentation by the major histocompatibility complex class I cytoplasmic domain. *Nat. Immunol.* 4: 1065–1073.
54. Steinman, R. M., D. Hawiger, K. Liu, L. Bonifaz, D. Bonnyay, K. Mahnke, T. Iyoda, J. Ravetch, M. Dhodapkar, K. Inaba, and M. Nussenzweig. 2003. Dendritic cell function in vivo during the steady state: a role in peripheral tolerance. *Ann. N. Y. Acad. Sci.* 987: 15–25.
55. Schurich, A., M. Berg, D. Stabenow, J. Böttcher, M. Kern, H. J. Schild, C. Kurts, V. Schuette, S. Burgdorf, L. Diehl, et al. 2010. Dynamic regulation of CD8 T cell tolerance induction by liver sinusoidal endothelial cells. *J. Immunol.* 184: 4107–4114.
56. Böttcher, J. P., O. Schanz, D. Wohlleber, Z. Abdullah, S. Debey-Pascher, A. Staratschek-Jox, B. Höchst, S. Hegenbarth, J. Grell, A. Limmer, et al. 2013. Liver-primed memory T cells generated under noninflammatory conditions provide anti-infectious immunity. *Cell. Rep.* 3: 779–795.
57. Nair, P., D. Amsen, and J. M. Blander. 2011. Co-ordination of incoming and outgoing traffic in antigen-presenting cells by pattern recognition receptors and T cells. *Traffic* 12: 1669–1676.
58. Clement, C. C., O. Rotzschke, and L. Santambrogio. 2011. The lymph as a pool of self-antigens. *Trends Immunol.* 32: 6–11.
59. Friedlaender, M. H., and H. Baer. 1972. Immunologic tolerance: role of the regional lymph node. *Science* 176: 312–314.
60. Thomas, S. N., J. M. Rutkowski, M. Pasquier, E. L. Kuan, K. Alitalo, G. J. Randolph, and M. A. Swartz. 2012. Impaired humoral immunity and tolerance in K14-VEGFR-3-Ig mice that lack dermal lymphatic drainage. *J. Immunol.* 189: 2181–2190.
61. Liao, S., G. Cheng, D. A. Conner, Y. Huang, R. S. Kucherlapati, L. L. Munn, N. H. Ruddle, R. K. Jain, D. Fukumura, and T. P. Padera. 2011. Impaired lymphatic contraction associated with immunosuppression. *Proc. Natl. Acad. Sci. USA* 108: 18784–18789.
62. Frew, A. J. 2010. Allergen immunotherapy. *J. Allergy Clin. Immunol.* 125(2, Suppl. 2): S306–S313.
63. Redmond, W. L., and L. A. Sherman. 2005. Peripheral tolerance of CD8 T lymphocytes. *Immunity* 22: 275–284.